Electronic Supplementary Material (ESI) for Journal of Materials Chemistry C.

Supporting Information

Templated synthesis of 1D Ag nanohybrid in the solid state and its organized network for strain-sensing application

Jize Liu,‡[a] Quanquan Guo,‡[a] Shizhe Mao[a], Zhenming Chen,[b] Xu Zhang,[a] Yibo Yang[a] and Xinxing Zhang[a]*

[a]State Key Laboratory of Polymer Materials Engineering, Polymer Research Institute of Sichuan University, Chengdu 610065, China

[b]Guangxi Key Laboratory of Calcium Carbonate Resources Comprehensive Utilization, College of Materials & Environmental Engineering, Hezhou University, Hezhou 542899, China

E-mail: xxzwwh@scu.edu.cn

**Corresponding author: Xinxing Zhang*
***E-mail address:** xxzwwh@scu.edu.cn*
Tel: +86-28-85460607 Fax: +86-28-85402465

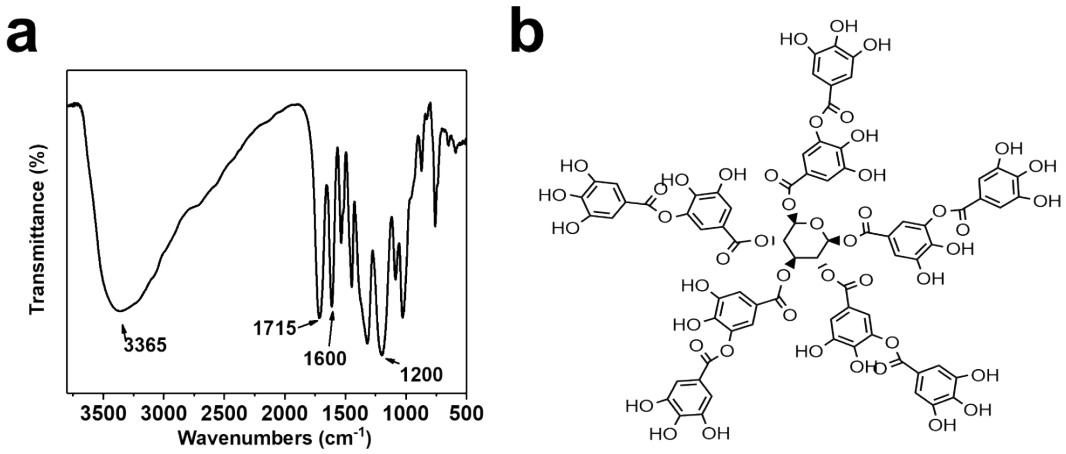

Figure S1. FT-IR spectra (a) of TA powder and its molecular structural formula (b).

As shown in **Figure S1b**, there are masses of phenolic hydroxyl groups in TA molecular, which are the basis of the strong reducing property and hydrogen-bonding anchoring effect. The TA powder exhibits typical characteristic peaks at approximately 3365 and 1200 cm^{-1} **(Figure S1a),** which are ascribed to phenolic hydroxyl groups. The characteristic peak at 1715 cm^{-1} is corresponding to the ester group attach to benzene ring and the three characteristic peaks at approximately 1600 to 1400 cm^{-1} are corresponding to the frame vibration of benzene ring. The masses of phenolic hydroxyl groups make TA possesses strong reducing property and chelating effect.[1-3]

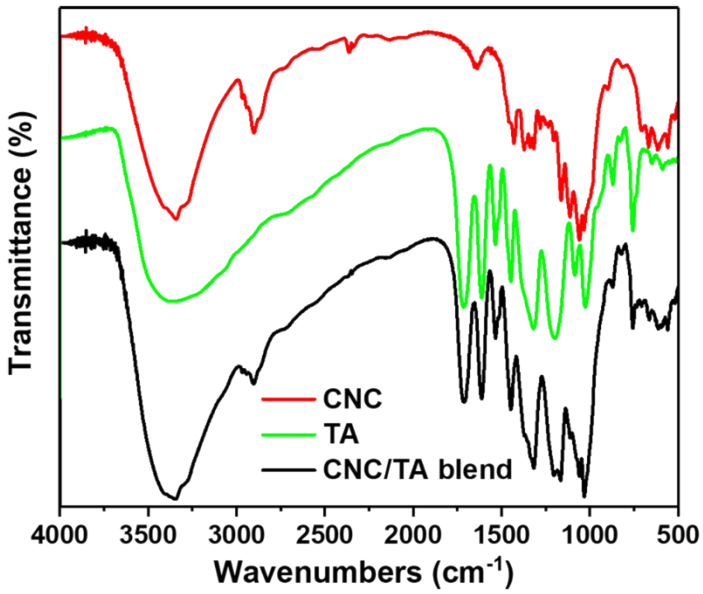

Figure S2. FT-IR spectra of CNC, TA and CNC/TA blend.

According to the FTIR spectra given in **Figure S2**, the curve of CNC exhibits typical characteristic peaks at approximately 1190 and 1071 cm^{-1} which are ascribed to sulfonic acid group of CNC.[4] The broad peak at approximately 3350 cm^{-1} is corresponding to the stretching vibration of −OH group. Such a strong and broad peak at approximately 3350 cm^{-1} indicates that there is a strong hydrogen-bonding between CNC and TA molecules. Meanwhile, these negatively charged functional groups on CNC and TA allow the chelation of Ag^{+} ions deposition in form of nanoparticles, resulting in a good stability and suspension dispersion ability of the obtained Ag@CNC nanohybrid.[5]

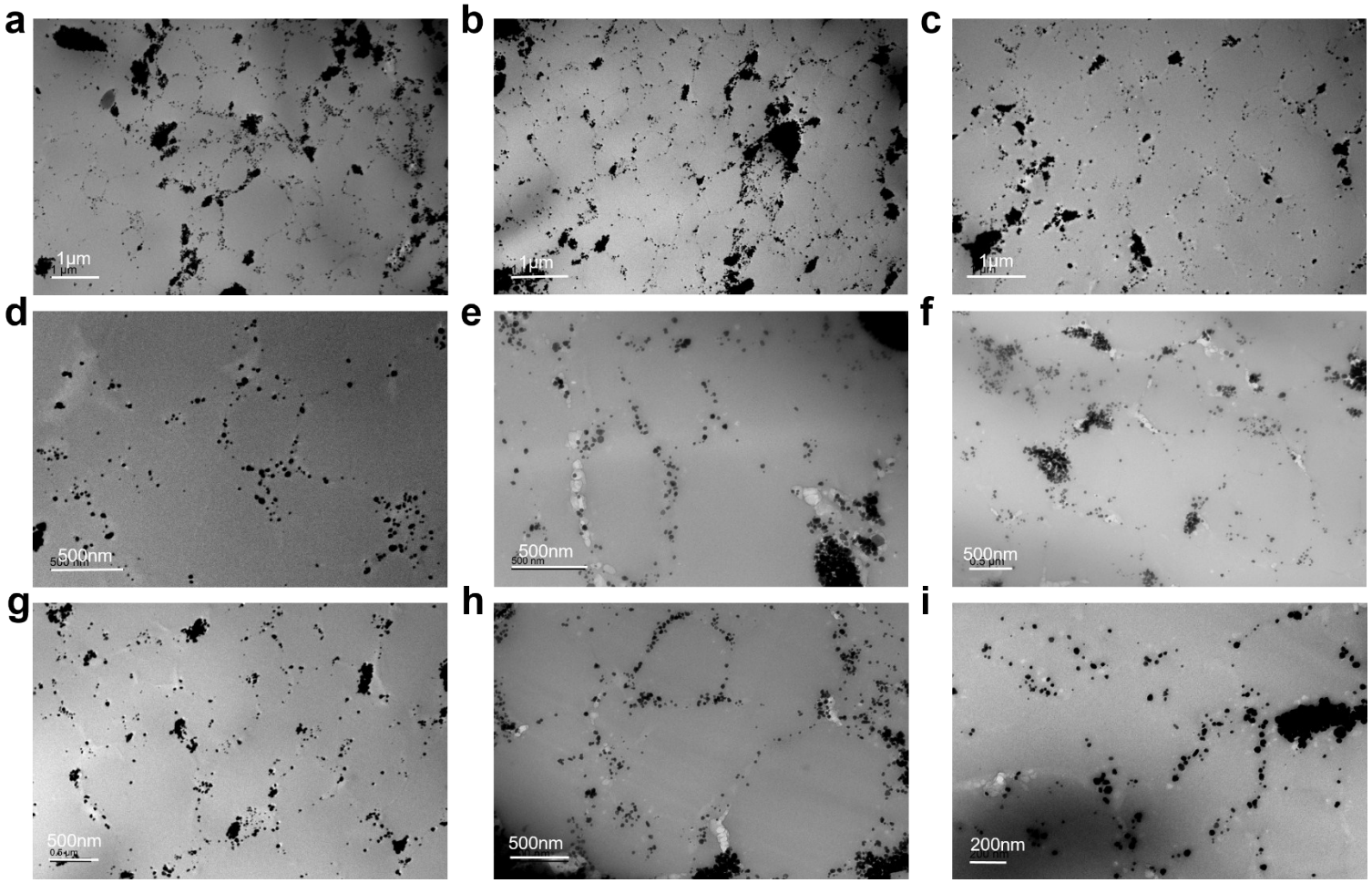

Figure S3. TEM images of the organized conductive network in Ag@CNC/ENR nanocomposite.

As depicted in **Figure S3**, the obtained Ag@CNC nanohybrids can assemble into an organized interconnected conductive network in rubber matrix with excellent dispersion and uniformity.

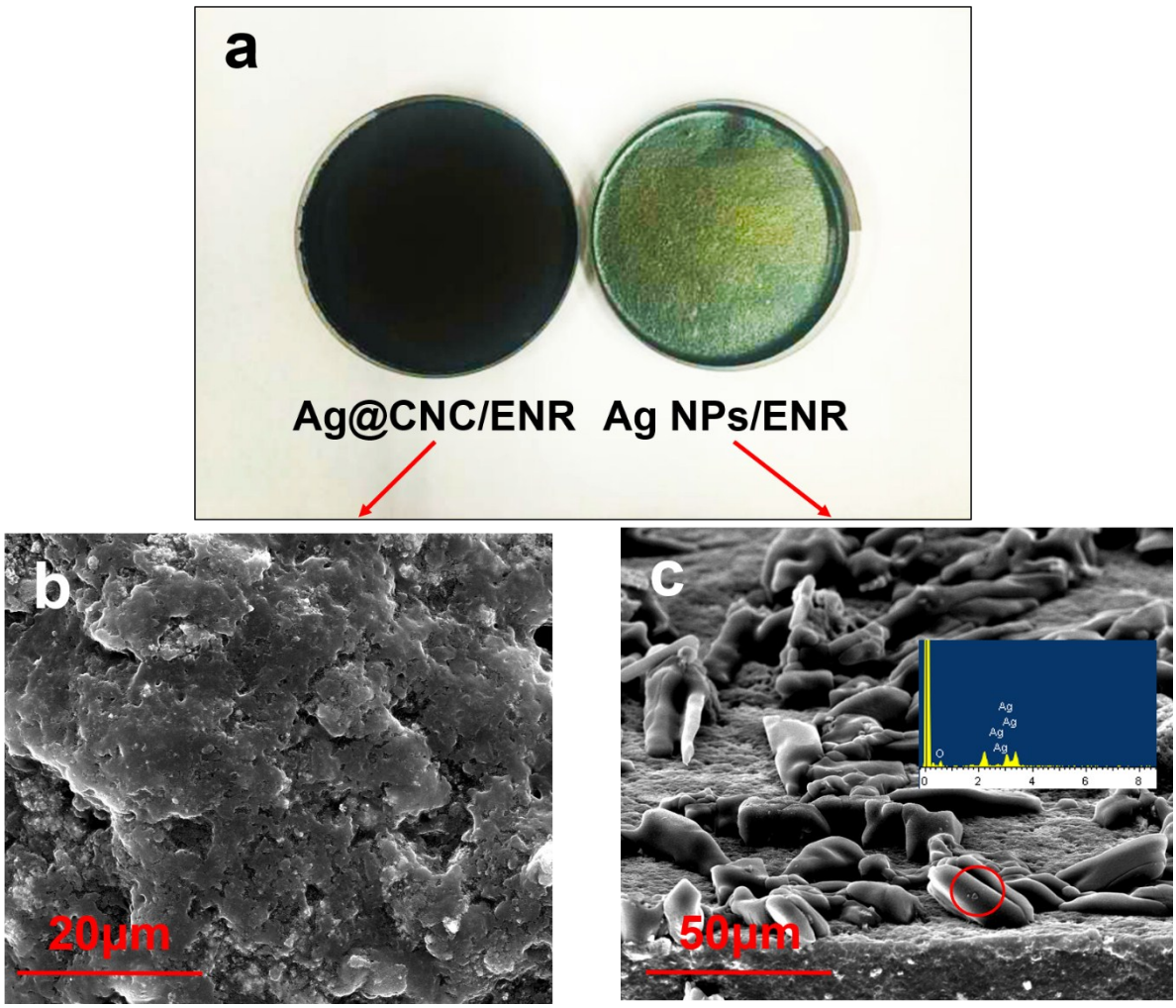

Figure S4. (a) Digital pictures of the obtained Ag@CNC/ENR nanocomposite (left) and Ag NPs/ENR composite before two-roll mill processing (right) with 1.8 vol% of Ag. SEM image of the surface morphology of Ag@CNC/ENR (b) and Ag NPs/ENR composite before tow-roll milling process with a corresponding EDS spectrum (c).

Ag NPs are tend to aggregate together during the preparation of polymer composites,[6] which greatly hinders the construction of a desired organized structure in polymer matrix. As shown in **Figure S4a**, there is no obvious metallic luster on the surface of Ag@CNC/ENR nanocomposite (left) contrast to Ag NPs/ENR (right), which suggest that our Ag@CNC 1D nanostructure prevents AgNPs from aggregation. To further illustrate the aggregation morphology of Ag NPs, SEM and EDS analysis was carried out (**Figure S4b and c)**. Here, obviously, Ag NPs/ENR composite without CNC shows

a mass of Ag aggregations at around 20 μm on the surface which is consistent with the result of **Figure S5a,** while there is no obvious aggregation on the surface of Ag@CNC/ENR. The results indicate that the existence of CNC plays an important role in preventing AgNPs from aggregation, which benefits to construct an organized conductive network in rubber matrix.

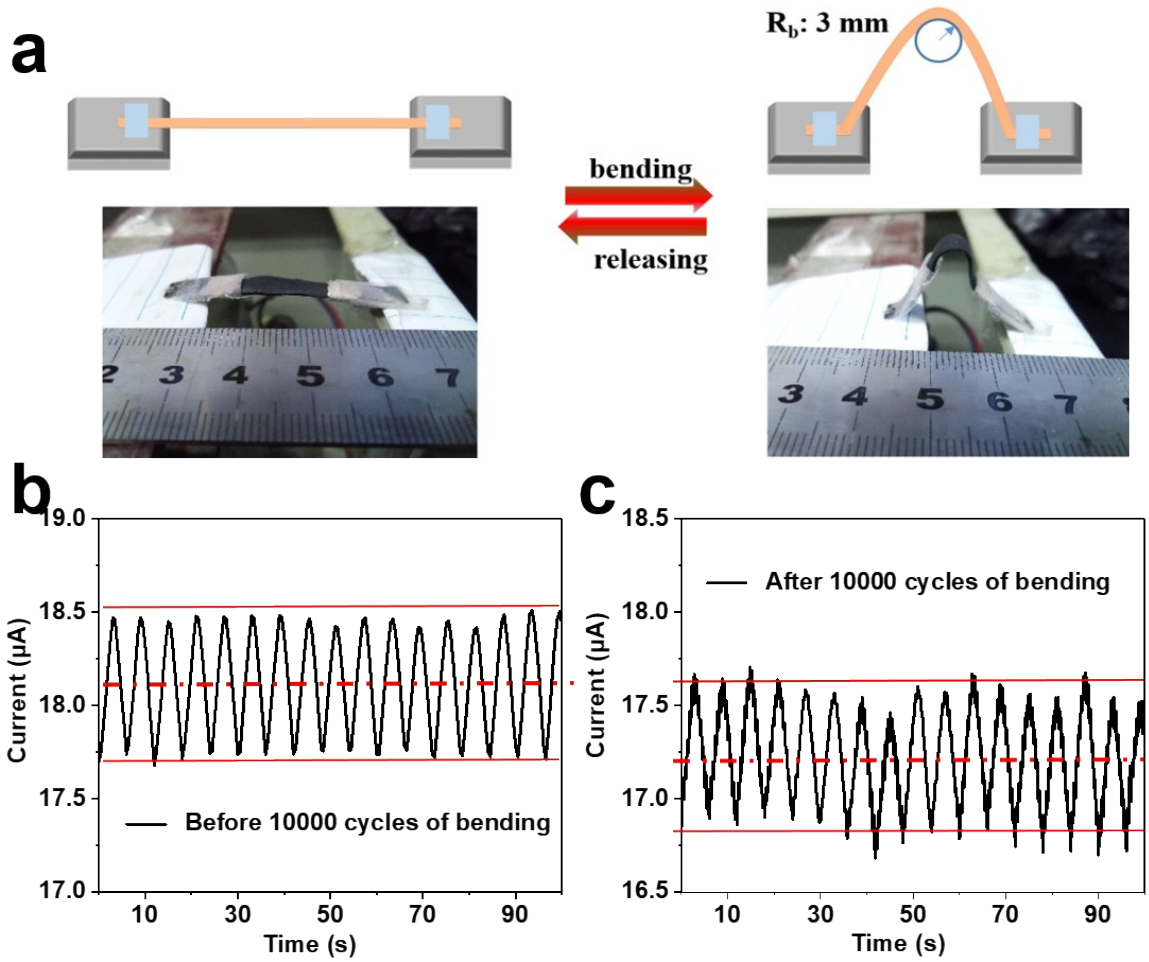

Figure S5. (a) Schematic illustration of the repeatedly bending process. Variation of electrical current of the obtained sensor with the fixed strains of 5% before (b) and after (c) 10000 cycles of bending.

As can be seen in **Figure S5b and c**, under a fixed voltage of 6 V, our strain senor exhibits an outstanding durability after experiencing 10 000 bending cycles. Here, a slight resistance change (5%) was indicated after 10 000 cycles with almost constant current change (which does not exceed 1 order of magnitude).

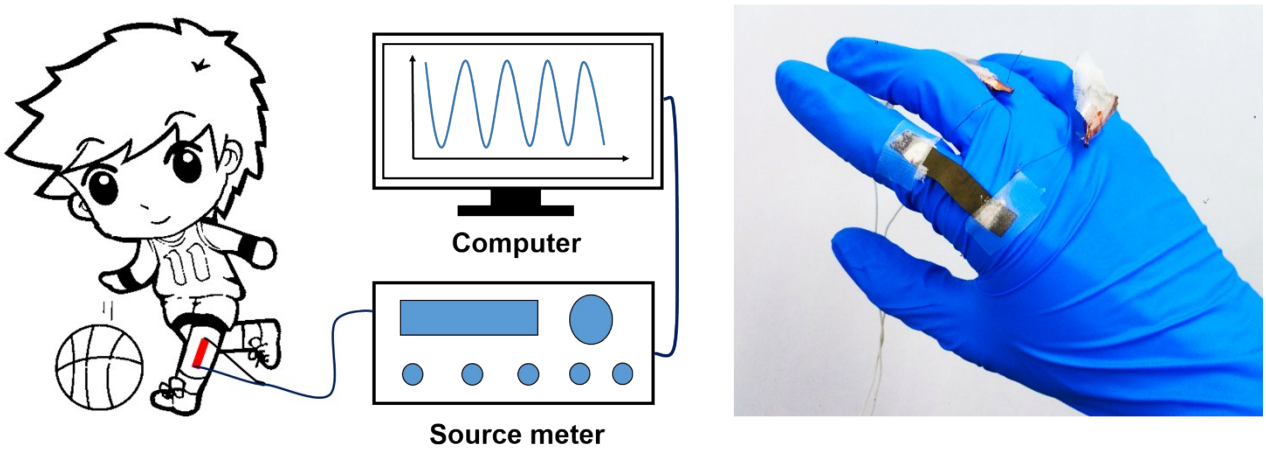

Figure S6. Schematic illustration of the motion monitoring based on our strain sensor and its manner of wearing.

There are three basic deformation types in practical applications, including stretching, light compression and great compression as shown in **Figure 6d**. When the sensor is stretched, the conductive pathways are destroyed and the resistance increases as a result. And when the sensors are compressed slightly, the rigid Ag@CNC conductive units joint in a tighter way, resulting in the reduction of resistance. However, when the sensors are greatly compressed, the deformation becomes larger, and the resistance increases again. These three basic deformation types and the change of resistance they bring are the basic units of different current variation.

Reference

1. E. B. a. M. O. zacar, *J. Am. Chem. Soc.*, 2009, **48**, 5686-5690.
2. X. Tian, J. Li and S. Pan, *J. Nanopart. Res.*, 2009, **11**, 1839-1844.
3. Y. Li, Y. Xie, Z. Wang, N. Zang, F. Carniato, Y. Huang, C. M. Andolina, L. R. Parent, T. B. Ditri, E. D. Walter, M. Botta, J. D. Rinehart and N. C. Gianneschi, *ACS Nano*, 2016, **10**, 10186-10194.
4. P. Lu and Y. L. Hsieh, *Carbohyd. Polym.*, 2010, **82**, 329-336.
5. X. Wu, C. Lu, Z. Zhou, G. Yuan, R. Xiong and X. Zhang, *Environ. Sci.-Nano.*, 2014, **1**, 71.
6. Z. Zhou, C. Lu, X. Wu and X. Zhang, *RSC Adv.*, 2013, **3**, 26066.